The Journal *of* Immunology

Divergent Phenotypes of Human Regulatory T Cells Expressing the Receptors TIGIT and CD226

This information is current as of December 1, 2016.

Christopher A. Fuhrman, Wen-I Yeh, Howard R. Seay, Priya Saikumar Lakshmi, Gaurav Chopra, Lin Zhang, Daniel J. Perry, Stephanie A. McClymont, Mahesh Yadav, Maria-Cecilia Lopez, Henry V. Baker, Ying Zhang, Yizheng Li, Maryann Whitley, David von Schack, Mark A. Atkinson, Jeffrey A. Bluestone and Todd M. Brusko

Supplementary Material	http://www.jimmunol.org/content/suppl/2015/05/20/jimmunol.1402381.DCSupplemental.html
References	This article **cites 48 articles**, 19 of which you can access for free at: http://www.jimmunol.org/content/195/1/145.full#ref-list-1
Subscriptions	Information about subscribing to *The Journal of Immunology* is online at: http://jimmunol.org/subscriptions
Permissions	Submit copyright permission requests at: http://www.aai.org/ji/copyright.html
Email Alerts	Receive free email-alerts when new articles cite this article. Sign up at: http://jimmunol.org/cgi/alerts/etoc

Divergent Phenotypes of Human Regulatory T Cells Expressing the Receptors TIGIT and CD226

Christopher A. Fuhrman,*,1 Wen-I Yeh,*,1 Howard R. Seay,* Priya Saikumar Lakshmi,* Gaurav Chopra,† Lin Zhang,* Daniel J. Perry,* Stephanie A. McClymont,† Mahesh Yadav,† Maria-Cecilia Lopez,‡ Henry V. Baker,‡ Ying Zhang,§ Yizheng Li,¶ Maryann Whitley,¶ David von Schack,§ Mark A. Atkinson,* Jeffrey A. Bluestone,‡ and Todd M. Brusko*

Regulatory T cells (Tregs) play a central role in counteracting inflammation and autoimmunity. A more complete understanding of cellular heterogeneity and the potential for lineage plasticity in human Treg subsets may identify markers of disease pathogenesis and facilitate the development of optimized cellular therapeutics. To better elucidate human Treg subsets, we conducted direct transcriptional profiling of CD4+FOXP3+Helios+ thymic-derived Tregs and CD4+FOXP3+Helios− T cells, followed by comparison with CD4+FOXP3−Helios− T conventional cells. These analyses revealed that the coinhibitory receptor T cell Ig and ITIM domain (TIGIT) was highly expressed on thymic-derived Tregs. TIGIT and the costimulatory factor CD226 bind the common ligand CD155. Thus, we analyzed the cellular distribution and suppressive activity of isolated subsets of CD4+CD25+CD127lo/− T cells expressing CD226 and/or TIGIT. We observed TIGIT is highly expressed and upregulated on Tregs after activation and in vitro expansion, and is associated with lineage stability and suppressive capacity. Conversely, the CD226+TIGIT− population was associated with reduced Treg purity and suppressive capacity after expansion, along with a marked increase in IL-10 and effector cytokine production. These studies provide additional markers to delineate functionally distinct Treg subsets that may help direct cellular therapies and provide important phenotypic markers for assessing the role of Tregs in health and disease. *The Journal of Immunology*, 2015, 195: 145–155.

The adaptive immune system provides the host with a vast receptor repertoire of T and B cells that facilitate protection from a wide array of pathogenic microbes. One consequence of this incredible diversity is the development of T and B cells specific for self-tissues (1). To counteract this autoreactivity, the immune system uses a number of mechanisms to reinforce peripheral immune tolerance, including a dominant role for a small population of CD4+ regulatory T cells (Tregs) (2). The requirement for regulation is most apparent in individuals presenting with a mutation in the Treg lineage transcription factor FOXP3, which results in fatal autoimmune disease (3).

Tregs exert their suppressive properties through a host of tolerogenic enzymatic pathways, cytokines, and the expression of multiple negative regulators (4). Of these, CTLA-4 and PD-1 regulate T cell activation through interactions with APCs and host tissues (5). Moreover, it is apparent that Tregs, like their Th counterparts, exhibit some level of lineage heterogeneity (6–8), as well as the potential for cellular plasticity in response to environmental cues (9). Deficiencies in Treg frequency and/or function have been associated with autoimmune diseases (10). Notably, we reported an increase in IFN-γ+Helios− Tregs with reduced suppressive capacity in type 1 diabetes (T1D) (11). An analogous finding was also reported in patients with MS (12). Unstable function has also been observed at a single-cell level, with IL-17–producing FOXP3+ Tregs exhibiting some suppressive capacity that was attenuated in the presence of inflammatory cytokines (13). Collectively, these studies raise the intriguing potential that subsets of Ag-experienced Tregs may contribute to defective immune regulation in the context of inflammation and autoimmune disease (9).

The ability to preserve and/or bolster the activity of Tregs is now appreciated as being key for inhibiting autoimmune reactivity (14). These studies have generally focused on two subsets of Tregs. Thymic-derived Tregs (tTregs) express the transcription factors FOXP3 and Helios and are demethylated at the FOXP3–Treg-

*Department of Pathology, Immunology and Laboratory Medicine, College of Medicine, University of Florida, Gainesville, FL 32610; †Department of Molecular Genetics and Microbiology, College of Medicine, University of Florida, Gainesville, FL 32603; ‡Diabetes Center and Department of Medicine, University of California, San Francisco, San Francisco CA 94143; §Precision Medicine–Bioanalytical, Pfizer, Cambridge, MA 02139; and ¶Pfizer Research and Development Business Technologies, Cambridge, MA 02139

1C.A.F. and W.Y. contributed equally to this work.

ORCIDs: 0000-0002-5364-6935 (C.A.F.); 0000-0003-2878-9296 (T.M.B.).

specific demethylated region (TSDR) (15). In contrast, peripher-ally induced Tregs develop from naive T cells under tolerogenic conditions and are minimally demethylated at the TSDR (16).

To further characterize the diversity of Tregs, we conducted a transcriptional profile of human T conventional cells (Tconvs), FOXP3^{+}Helios^{−} T cells, and FOXP3^{+}Helios[+] tTreg subsets. Through this analysis, we demonstrate that the coinhibitory mol-ecule TIGIT is highly expressed in tTregs. TIGIT competes with the costimulatory molecule CD226 for binding to the poliovirus receptor/Nectin-like-5/CD155 prominently expressed on APCs (17). *CD226* has been identified as an autoimmune suscepti-bility gene, with a single nucleotide polymorphism (Gly[307]Ser; rs763361) linked to T1D, multiple sclerosis, rheumatoid arthritis, systemic lupus erythematosus, Wegner's granulomatosis, celiac disease, and juvenile idiopathic arthritis (18, 19). This recently described axis shares many parallel functions with the CD28–CTLA-4 pathway in terms of promoting or inhibiting T cell ac-tivation, respectively (20–22). Activation of CD226 leads to TCR association and activation that promotes Th1-related signaling (22, 23). Phosphorylation of the tyrosine at residue 322 results in IFN-γ secretion and proliferation (24). In contrast, TIGIT contains an inhibitory ITIM that leads to SHIP1 recruitment and down-modulation (20, 25). Ligation of TIGIT with an agonistic Ab has been shown to suppress activation (22).

TIGIT has recently been associated with Treg biology through transcriptional profiling of Tregs (8, 21, 26, 27), and has also been characterized as highly demethylated in FOXP3^{+} T cells (28). In addition to intrinsic inhibitory activity, TIGIT binding to CD155 on dendritic cells leads to a reduction in IL-12p40 and a con-comitant increase in IL-10 production (29). Importantly, TIGIT attenuates antitumor immunity by CD8^{+} T cells (30), and it was recently demonstrated as a mechanism by which Tregs exert their suppressive activity (31).

Despite the roles of this costimulatory axis in immunoregulation, little is known about the cellular distribution and phenotype of human Tregs expressing CD226 and TIGIT. In this study, we sought to address this knowledge void and specifically understand the role of TIGIT and CD226 in Treg biology. To that end, we isolated subsets of CD4^{+}CD25^{+}CD127^{−/lo} Tregs expressing CD226 and/or TIGIT, and expanded them ex vivo to assess their phenotype and suppressive capacity. We demonstrate that production of IFN-γ within Tconvs and Tregs is tightly linked to coexpression of CD226. Conversely, selection of CD226^{−} Tregs, irrespective of initial TIGIT expression, leads to a suppressive population of tTregs that are demethylated at the TSDR.

Materials and Methods
Sample procurement and processing

Peripheral blood was collected from healthy control donors (median age 28.8, range 22.5–46.7) after informed consent in accordance with the In-stitutional Review Boards at the University of Florida and University of California, San Francisco or purchased from Life South Blood Centers (median age 23 y, range 20–26 y). Venous blood was collected in sodium-heparinized Vacutainer tubes (BD Biosciences) or supplied in sodium citrate followed by PBMC isolation by density gradient centrifugation. For FACS experiments, whole blood was pre-enriched by negative selection with RosetteSep (Stemcell) before centrifugation.

Transcription factor sorting and expression analysis

CD4^{+} RosetteSep-enriched T cells were stained with anti-CD4, fixed, and permeabilized with the FOXP3 Fix/Perm (Biolegend) per manufacturer's recommendations and stained for FOXP3 and Helios. tTregs (CD4^{+} FOXP3^{+}Helios^{+}), CD4^{+}FOXP3^{+}Helios^{−} T cells, and Tconvs (CD4^{+} FOXP3^{−}Helios^{−}) were sorted into RNALater (Life Technologies). RNA was extracted with the RNeasy FFPE Kit (Qiagen) by proteinase K di-gestion followed by incubation at 80°C. RNA quality was verified on

a Bioanalyzer (>300 bp length for >50% of transcripts) with the RNA Nano Chip (Agilent Technologies). RNA transcripts (100 ng) were directly quantified with the nCounter and the Human Immunology GX Panel (v1; NanoString Technologies).

Flow cytometry and FACS

All samples were first stained with Fixable Live/Dead Yellow or Near IR (Invitrogen). Surface markers were analyzed immediately after staining or after fixation with BD Cytofix (BD Biosciences). Cells were stained for intracellular proteins in FOXP3 fixation and permeabilization buffers according to the manufacturer's protocol (Biolegend). Abs used included CD4-Pacific Blue (RPA-T4), TIGIT-APC or –PerCP-eFluor710 (MBSA43; eBioscience), CD4-PE-CF594 (RPA-T4), CD45RO-APC (UCHL1) and CD8 (SK1; BD Biosciences), CXCR3-PerCP-Cy5.5 (G025H7), CCR4-PE-Cy7 (TG6/CCR4), CCR6-BV605 (G034F3), CD226-PE (11A8), CD127-PE or -BV421 (A019D5), CD25-APC or –Alexa Fluor (AF) 488 (BC96), IFN-γ–PE-Cy7 (4S.B3), Helios-PE or -Pacific Blue, -AF647 (22F6), and FOXP3-AF488 and -PE (206D) (Biolegend).

Cytometric analyses were performed on a LSR Fortessa (BD Bio-sciences). Data were collected using BD DIVA acquisition software and imported into FlowJo (v9.7.5; Tree Star) for analysis. Marker positivity was determined by fluorescence minus one method. Expression levels were calculated with geometric mean fluorescence intensity (gMFI).

Cell sorting was conducted on a FACSAria III (BD Biosciences). Tregs (CD4^{+}CD25^{+}CD127^{−}) and Tconvs (CD4^{+}CD127^{+}) were further enriched based on CD226 and/or TIGIT expression. Postsort purities were typically >93% (median 93%; range 90–95%).

In vitro T cell expansion and activation cultures

Tregs and Tconvs were expanded as previously described (32). After ex-pansion, cells were analyzed for intracellular IFN-γ by reactivation for 4 h with PMA (10 μg/ml) and ionomycin (500 nM) in the presence of GolgiStop (4 μl/6 ml culture; BD Biosciences). For multiplex cytokine detection, cells were activated with anti-CD3– and anti-CD28–coated dynabeads (Life Technologies) according to manufacturer recom-mendations, and supernatants were collected at 24, 48, and 72 h.

Suppression assays

Expanded Treg subsets were tested for their ability to suppress autologous T cell proliferation, as described previously (33), with the following modifications. Tregs were labeled with CFSE (0.15 μM), whereas responding cells were stained with Cell Trace Violet (2.5 μM; Life Technologies) and activated with either autologous APCs or Treg Sup-pression Inspector beads (Miltenyi Biotec). Triplicate cultures were har-vested and pooled after 96 h, stained with live/dead dye, CD4, CD8, CD226, and TIGIT, and proliferation was calculated by division index of gated live lymphocytes.

Analysis of the FOXP3-TSDR

TSDR demethylation at the conserved noncoding region 2 of *FOXP3* is a hallmark of lineage-stable tTregs (34). Nucleotides were isolated with AllPrep DNA/RNA Mini Kit (Qiagen) or DNeasy tissue kit (Qiagen), as appropriate. Bisulfite treatment of genomic DNA was performed on 500 ng DNA with the EZ DNA Methylation Kit (Zymo Research).

Real-time PCR was performed to determine the methylation status at the FOXP3-TSDR for each sample. DNA standards originated from unme-thylated bisulfite-converted human EpiTect control DNA (Qiagen) or universally methylated bisulfite-converted human control DNA (Zymo Research). To obtain a large quantity of standard, we PCR-amplified the TSDR using the following reaction: 50 μl reaction volume containing 25 μl of ZymoTaq PreMix buffer (Zymo Research) and 0.5 μM each of the primers FOXP3_TSDRfwd (5′-ATATTTTTAGATAGGGATATGGAGAT-GATTTGTTTGG-3′) and FOXP3_TSDRrev (5′-AATAAACATCACCT-ACCACATCCACCAACAC-3′). After incubation at 95°C for 10 min, amplification was performed as follows: 50 cycles at 95°C for 30 s, 55°C for 30 s, and 72°C for 1 min. Amplified PCR products were purified with the QIAquick Gel Extraction Kit (Qiagen). The concentration of purified control TSDR DNA was determined with a GE NanoVue spectropho-tometer (GE Healthcare Life Sciences).

TSDR real-time PCR was performed with probes that targeted meth-ylated or demethylated target sequences. The reaction was performed in 384-well white trays with a Roche LightCycler 480 system (Roche Diagnostics). Each reaction contained 10 μl LightCycler 480 Probes Master Mix (Roche), 1 μl bisulfite converted DNA sample or standards, 1 μM of each primer, and 150 nM of each probe with a final reaction value of 20 μl. The probes used for amplification were TSDR-Forward 5′-

GGTTTGTATTTGGGTTTTGTTGTTATAGT-3′ and TSDR-Reverse 5′-CTATAAAATAAAATATCTACCCTCTTCTCTTCCT-3′. The probes for target sequence detection were FAM-labeled methylated probe, FAM-CGGTCGGATGCGTC-MGB-NFQ, or VIC-labeled unmethylated probe, VIC-TGGTGGTTGGATGTGTTG-MGB-NFQ. All samples were tested in triplicate. The protocol for real-time amplification is as follows: after initial denaturation at 95°C for 10 min, the samples were subjected to 50 cycles at 95°C for 15 s and at 61°C for 1 min. Fourteen different ratios of fully methylated and demethylated template were used as real-time standards. A six-order polynomial equation was used to extrapolate the percentage of cells demethylated at the TSDR for each sample.

T cell transcriptional profiling

Using the nSolver Analysis Software (NanoString), counts were first normalized to the geometric mean of the positive control spiked into the assay, then normalized to 10 housekeeping genes built into the array. Subsequent analyses were conducted with the Partek Genomic Suite (Partek). The signal-to-noise ratio was significantly higher in the expanded T cell counts compared with the fixed cell sorted T cell counts. Thus, two different statistical approaches were used.

For the mRNA count data from fixed cells, counts were normalized to the 10 internal housekeeping genes, and the average of the background counts (noise) was subtracted with values lower than background set to 1. The fold change was calculated by taking the geometric mean of the counts, then dividing one subset by another. A paired ANOVA coupled with the Bonferroni multiple test correction (MTC) was used to determine differentially regulated genes with a significance value of $p < 0.05$. Complete gene expression data can be found by accessing Gene Expression Omnibus [GEO] accession number: GSE61834; http://www.ncbi.nlm.nih.gov/geo/).

For the mRNA from expanded cells, genes that were below the background threshold (mean of negative controls count + 2 SDs) for both Tregs and Tconvs were removed from the analysis. Because Tconvs often have a variance different from Tregs at both the RNA and the proteins levels, a Welch's ANOVA with a Bonferroni MTC was used to determine significance ($p < 0.05$). Significantly regulated genes with a false discovery rate <0.05 were normalized around zero and clustered using the average of the means. Eighty-two genes were identified as being differentially expressed between the populations (GEO accession number GSE62015).

Isolation of IFN-γ–producing Tregs

Tregs and Tconvs were FACS isolated from five healthy subjects (median age 26 y, range 22–30 y) and sorted into two groups. In brief, the first group was stimulated for 4 h with PMA/ionomycin and labeled with the IFN-γ cytokine cell-capture reagent (Miltenyi Biotech) followed by FACS isolation of IFN-γ⁻ and IFN-γ⁺ populations, as previously described (11). The second set was expanded to day 14 before reactivation and cytokine cell capture.

For each sample, 25 ng total RNA was amplified using the Ovation Pico WTA System (NuGen) and labeled with Encore Biotin Module V2 (NuGen). GeneChip Human Genome U133 Plus 2.0 arrays (Affymetrix) were hybridized to 5 μg labeled, amplified cDNA, washed, stained, and scanned according to the protocol described in the GeneChip Expression analysis manual (GEO accession number GSE59786). Gene expression profiling data were extracted from the Affymetrix Microarray Suite 5.0 (MAS 5.0) software and used for subsequent statistical analyses.

Multiplex cytokine assay

Cytokine production was determined using the Human T_H17 Magnetic Bead Panel (HT17MG-14K-PX25; EMD Millipore) according to manufacturers' instructions from culture supernatants collected and run in duplicate. Samples were processed on a Bio-Tek ELx405, detected with MAGPIX system (EMD Millipore), and analyzed with Milliplex Analyst software.

Data analysis

An ANOVA with a post hoc Tukey MTC was used for analysis of cytometric data using Prism (v6; GraphPad). Geister–Greenhouse variance correction method was applied to the data to account for the difference in variance between Tregs and Tconvs, with values matched between each individual.

Results

TIGIT is enriched in tTregs

Human Tregs display a considerable degree of heterogeneity (15). To limit biases for putatively identified surface markers, we FACS-sorted Tregs after intracellular staining for FOXP3 and

Helios. We sorted Tconv (FOXP3⁻Helios⁻), FOXP3⁺Helios⁻, and tTreg subsets (FOXP3⁺Helios⁺; Fig. 1A), which then underwent direct mRNA hybridization that facilitates the direct quantitation of mRNA transcripts without reverse transcription and amplification. This approach is compatible with partially degraded RNA samples, such as those obtained from fixed samples (35).

Patient-to-patient variance accounted for 77% of the expression differences observed between the samples; however, we identified genes putatively associated with Tregs, including CTLA-4 and IL2RA (Supplemental Table I) (36). Specifically, we found the mRNA levels of TIGIT to be 12.4 times greater in tTregs compared with Tconvs ($p < 0.05$; Fig. 1B). In addition, our analysis demonstrated strong coexpression of TIGIT and Helios in CD4⁺ FOXP3⁺ T cells (Fig. 1C). Our results are in line with prior reports suggesting that TIGIT expression is maintained by FOXP3 (28) and supports the notion that it may play an important role in immune regulation (20, 21, 29, 31).

Given that TIGIT and CD226 compete for binding to the ligand CD155 (21, 22), we analyzed their surface expression on CD4⁺ T cells in combination with FOXP3 and Helios (Fig. 2). Strikingly, tTregs had the highest percentage of TIGIT⁺ cells (83.4 ± 6.2%) and did not express CD226 in the absence of TIGIT (Fig. 2A). In contrast, Tconvs coexpressed TIGIT only with high CD226 expression, suggesting TIGIT may play an important role in Tconvs after activation, as noted previously (22). TIGIT expression by tTregs was increased in frequency and gMFI compared with FOXP3⁺Helios⁻ T cells, and the lowest frequency of TIGIT⁺ cells and gMFI found in Tconvs (Fig. 2B, *left graphs*). In contrast, CD226 expression was higher in Tconvs, followed by FOXP3⁺ Helios⁻, and then tTregs (Fig. 2B, *right graphs*). FOXP3⁺Helios⁻
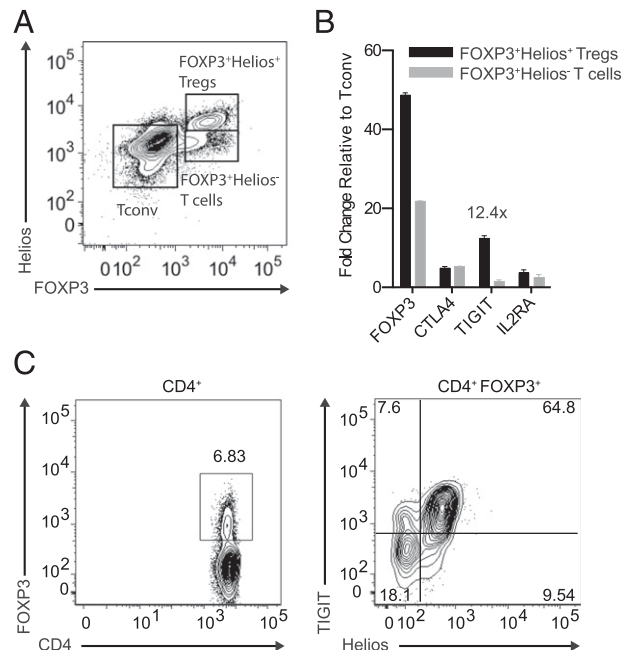

FIGURE 1. TIGIT expression is enriched in FOXP3⁺Helios⁺ Tregs. CD4⁺ T cells were enriched from peripheral blood by negative selection and stained for CD4 and the intracellular transcription factors FOXP3 and Helios. (**A**) Cells were isolated by FACS to yield Tconvs (*lower left gate*), FOPX3⁺Helios⁻ T cells (*lower right gate*), and FOXP3⁺Helios⁺ Tregs (*upper right gate*), with representative populations shown. RNA was isolated from sorted populations and subjected to direct transcriptional profiling on the Human Immunology GX Panel on the NanoString platform. (**B**) TIGIT expression was 12.4-fold higher in FOXP3⁺Helios⁺ Tregs compared with Tconvs ($n = 3$, $p < 0.05$). (**C**) Representative TIGIT and Helios expression was shown in gated CD4⁺FOXP3⁺ T cells.

FIGURE 2. Differential expression of CD226 and TIGIT on CD4$^+$ T cell subsets. PBMCs were stained for CD4, CD226, TIGIT, and the transcription factors FOXP3 and Helios. (**A**) Representative plots show TIGIT and CD226 on total CD4$^+$ T cells, Tconv, FOPX3$^+$Helios$^-$, and FOXP3$^+$Helios$^+$ Treg populations. (**B**) Graphs show summarized data demonstrating TIGIT is enriched in Treg populations (*left graphs*) analyzed by gMFI and percent positive, whereas CD226 is enriched in Tconvs (*right graphs*). Shown are mean ± SE with significance indicated ($n = 5$; *$p < 0.05$, ***$p < 0.001$, ****$p < 0.0001$). n.s., not significant.
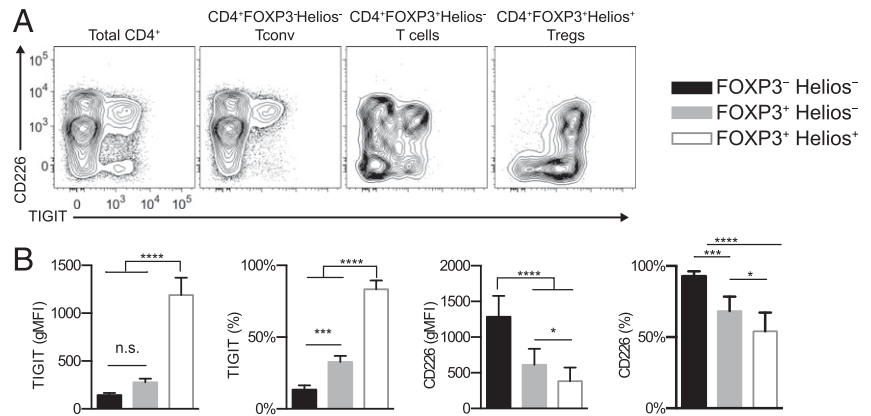
T cells demonstrated an intermediate phenotype for CD226 and TIGIT expression. Notably, we also analyzed CD96 (T cell activation, increased late expression [TACTILE]), a ligand that also binds CD155. CD96 expression positively correlated with CD226 but did not demonstrate the dynamic range observed for CD226 (data not shown). Hence we limited our downstream analyses to TIGIT and CD226.

Differentiated T cells concomitantly express high CD226 and chemokine receptors

Prior reports suggest signaling through CD226 suppresses Th2 differentiation and promotes Th1 responses and IFN-γ secretion (22). We sought to understand the cellular distribution and expression profiles of CD226 and TIGIT on human naive, central and effector memory, and T effector memory CD45RA$^+$ (TEMRA) subsets (Fig. 3A). Although naive T cells were the most abundant population in our cohort (mean ± SEM, 44.8 ± 14.6%), they expressed the lowest surface levels of CD226 (495.4 ± 73.5 gMFI), when compared with effector memory T cell (T$_{EM}$) and central memory T cell (T$_{CM}$) subsets (1785 ± 357.2 and 3185 ± 492.6, respectively; Fig. 3B). Furthermore, the cellular distribution of CD226 in the bulk CD4$^+$ T cell population demarcates naive (CD226$^{-/low}$) versus CD226^{hi} memory subsets. Few naive cells express TIGIT (5.3 ± 2.6%) compared with the memory subsets (29.0 ± 3.5% for T$_{EM}$ and 32.7 ± 8.2% for T$_{CM}$). Notably, one subject with a prominent TEMRA population was CD226^{hi}TIGIT$^-$ (Fig. 3A), which coincides with their role as a proinflammatory T cell subset (37).

In addition to robust CD226 expression in T$_{EM}$ and T$_{CM}$, we also noted that chemokine receptors expressed by Th2, Th17, and Th1 cells were coexpressed with high levels of CD226 (Fig. 3C, *upper plots*). TIGIT$^+$ populations also expressed chemokine receptors, albeit to a lesser extent than with CD226 (Fig. 3C, *lower plots*). Increased CD226 and TIGIT on differentiated subsets were observed for both CD4$^+$CD127$^+$ Tconvs and CD4$^+$CD25$^+$CD127$^{-/lo}$ Tregs (Fig. 3D).

CD226 expression is associated with effector cytokine production

CD226 and TIGIT have opposing roles in the regulation of IFN-γ (22). We sought to determine how CD226 and TIGIT influenced IFN-γ production by PBMCs after activation (Fig. 3E). IFN-γ tracked primarily to the CD226^{hi}TIGIT$^-$ fraction, with the CD226^{hi}TIGIT$^+$ population consistently containing a minor population of IFN-γ$^+$ T cells (64.7 ± 8.7 versus 24.9 ± 8.3%; $p = 0.011$). IFN-γ was coexpressed with CD226, as CD226^{int}TIGIT$^-$ and CD226^{int}TIGIT$^+$ populations contained significantly lower percentages of IFN-γ$^+$ cells than their CD226^{hi} counterparts

(Fig. 3F; 7.03 ± 3.29 and 3.42 ± 1.03%, respectively). The CD226$^-$ subset was largely devoid of IFN-γ$^+$ T cells (0.183 ± 0.053%). Overall, these results demonstrate a close association between CD226 and the production of IFN-γ by Ag-experienced T cells.

To determine whether this association was influenced by Th1-skewing conditions, we activated T cells in the presence of IL-12 (Supplemental Fig. 1). Although it has been previously shown that both CD226 and TIGIT increase upon T cell activation (22), the change in TIGIT expression by tTregs has not been characterized after culture with IL-12. As shown previously, CD226 expression increased over the 72-h time course (Supplemental Fig. 1A). Likewise, our data demonstrated that TIGIT increases after TCR activation (22). Notably, we observed TIGIT upregulation was attenuated by IL-12 in FOXP3$^+$Helios$^+$ Tregs (Supplemental Fig. 1B). IL-12 upregulated CD226 and IFN-γ as expected (Supplemental Fig. 1C, 1D); however, the proportion of tTregs recovered from the culture decreased in IL-12 (Supplemental Fig. 1E) (38). These data suggest a mechanism whereby IL-12 exposure may potentiate Tconv cytokine production concomitant with a reduction in both tTreg proliferation and TIGIT expression.

Our prior studies demonstrated elevated IFN-γ$^+$ Tregs in patients with T1D (11). To further characterize this subset, we isolated IFN-γ$^+$ or IFN-γ$^-$ Treg and Tconv subsets, and conducted a transcriptional profile of the FACS isolated subsets. Principal component analysis (PCA) indicated clear divergence of Treg and Tconv populations, with further discordance in IFN-γ$^+$ and IFN-γ$^-$ Tregs (Fig. 3G). Importantly, both freshly isolated and expanded IFN-γ$^+$ Tregs express significantly more CD226 than the IFN-γ$^-$ Treg subset (Supplemental Fig. 2A). Moreover, TIGIT expression was increased in IFN-γ$^-$ Tregs compared with IFN-γ$^+$ Tregs, whereas the inverse is true for Tconvs (Supplemental Fig. 2B).

CD226 and TIGIT identify functionally distinct subpopulations of Tregs

Human CD4$^+$CD25^{hi}CD127$^-$ Tregs contain a significant degree of heterogeneity in terms of lineage diversity and Ag exposure. We subdivided CD4$^+$CD25^{hi}CD127$^-$ Tregs (39) based on CD226 and TIGIT expression (Fig. 4A, *right plot*). FOXP3-TSDR demethylation at the conserved noncoding sequence 2 has been previously associated with Treg stability (34, 40). Hence we measured the percentage of cells demethylated at the TSDR in our subsets. When analyzed directly ex vivo, we observed CD226$^+$TIGIT$^-$ T cells were reduced in TSDR demethylation (30.0 ± 8.3%), in comparison with the other Treg subsets and Tconvs (Fig. 4B). Despite this reduction in TSDR demethylation, the resulting
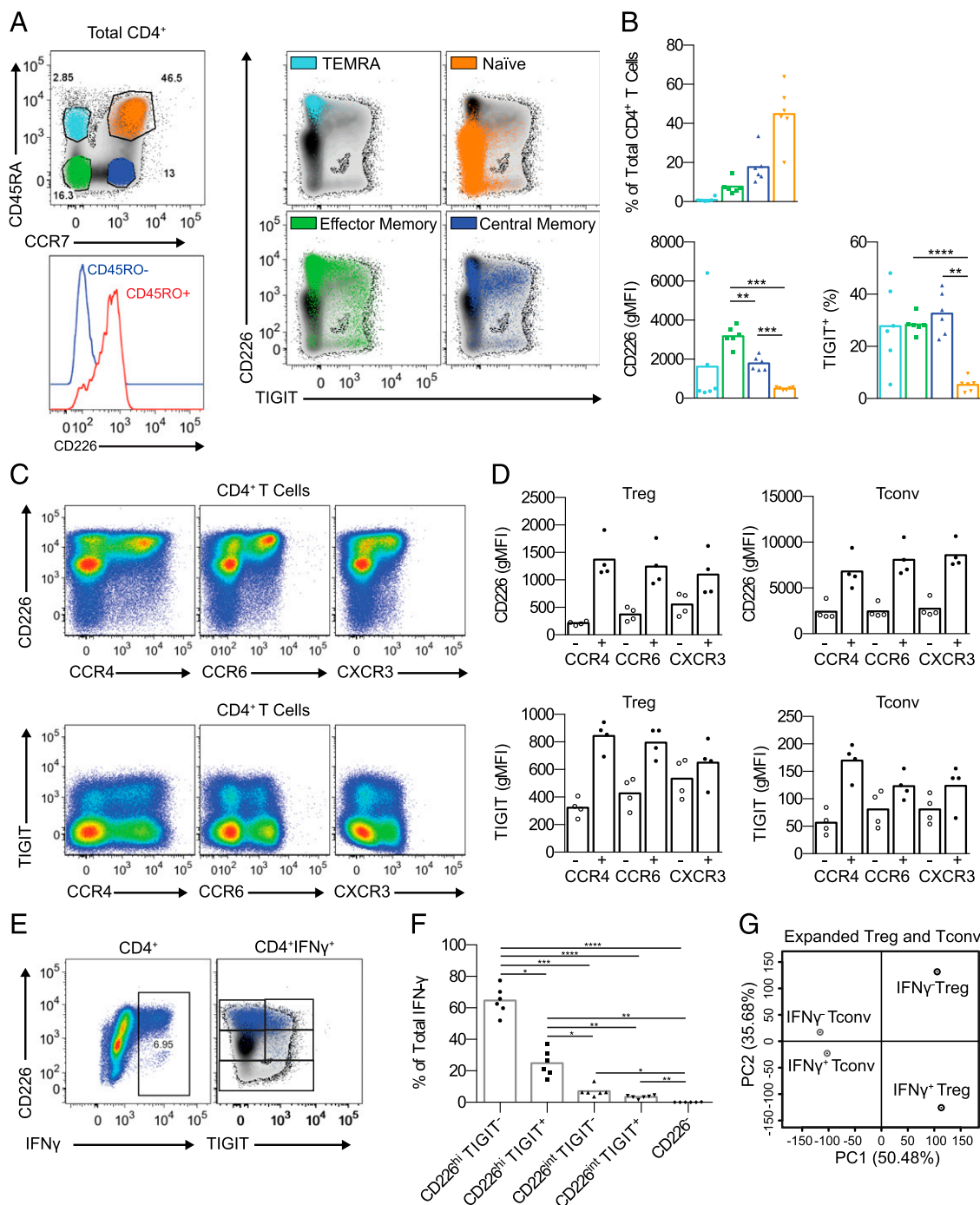
FIGURE 3. High CD226 expression is associated with a memory CD4$^+$ T cell phenotype. Cryopreserved PBMCs were thawed and stained for CD4, CCR7, CD45RA, CD45RO, CD226, and TIGIT or stimulated with PMA/ionomycin in the presence of monensin followed by intracellular staining of IFN-γ. (**A**) A representative plot shows gated viable CD4$^+$ naive T cells (orange), central memory (dark blue), effector memory (green), and T$_{EM}$ CD45RA$^+$ (TEMRA) (cyan) populations, and their TIGIT/CD226 expression compared with total CD4$^+$ T cells. A representative overlaid histogram shows CD226 expression on CD4$^+$ T cells as a function of CD45RO expression. (**B**) Data from six subjects are summarized for frequency, CD226 gMFI, and percent TIGIT$^+$ for each subset. (**C**) Cryopreserved PBMCs were thawed and stained for CD4, CD226, TIGIT, and the subset-specific chemokine receptors CCR4 (Th2), CCR6 (Th17), and CXCR3 (Th1). (**D**) Data from four subjects are summarized for Tregs (CD4$^+$CD25$^+$CD127$^{-/lo}$) and Tconvs (non-Tregs) and bifurcated by chemokine receptor expression. (**E**) Representative plots demonstrate that IFN-γ$^+$ cells are predominantly CD226^{hi} (*left plot*) and are less frequent in TIGIT$^+$ cells (*right plot*). (**F**) Summarized data of six subjects show CD226 and TIGIT expression on IFN-γ$^+$ populations. (**G**) Cytokine capture assays allowed the isolation of Tregs and Tconv subsets based on IFN-γ production capacity. Expanded cells were restimulated with PMA/ionomycin and analyzed by microarray (*n* = 5). IFN-γ$^+$ and IFN-γ$^-$ Tregs expanded into two distinct populations that could be distinguished from Tconvs as shown by PCA analysis. *$p < 0.05$, **$p < 0.01$, ***$p < 0.001$, ****$p < 0.0001$.

population suppressed to comparable levels when compared with the other freshly isolated CD4$^+$CD25^{hi}CD127$^-$ Treg populations (Fig. 4C). Dye dilution analysis facilitated further analysis of Treg proliferation and viability. We noted increased proliferation of

both the CD226$^-$TIGIT$^-$ (naive) and the CD2226$^+$TIGIT$^-$ populations. Interestingly, we noted increased IL-10 in the suppression assay coculture with CD2226$^+$TIGIT$^-$ Tregs. We also observed a trend toward more CD2226$^+$TIGIT$^+$ cell death; how-
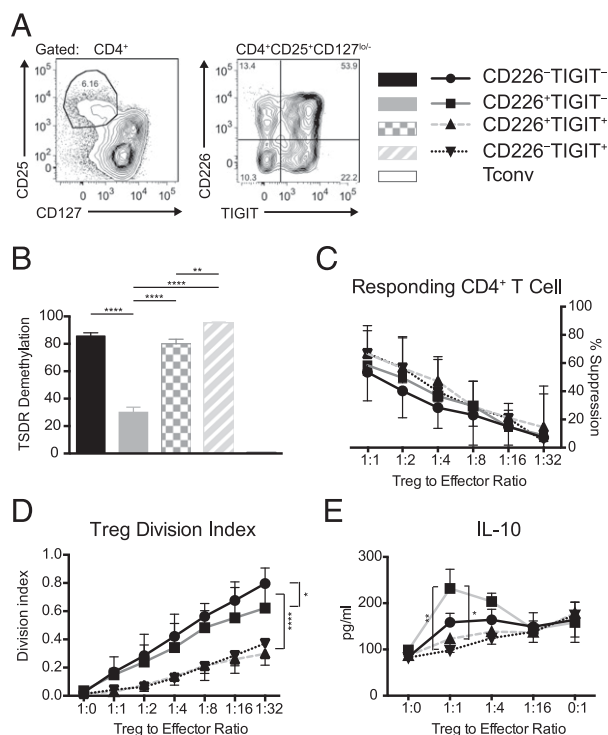
FIGURE 4. Direct ex vivo analysis of TIGIT and CD226 Tregs. (**A**) CD4⁺CD25⁺CD127⁻ T cells were sorted by FACS and further subdivided based on TIGIT and CD226 expression. (**B**) Freshly sorted Treg subsets were analyzed for FOXP3-TSDR demethylation. (**C**) Treg subsets and autologous Tconvs were stained with distinct proliferation dyes and cultured at indicated ratios in the presence of Treg suppression Inspector beads for 4 d. Percent suppression was calculated by division index of CD4⁺ Tconvs in coculture relative to Tconvs alone. (**D**) The proliferation of each Treg subset was shown in the division index. (**E**) IL-10 production in suppression assay coculture supernatants at indicated Treg/Tconv ratios. $*p < 0.05$, $**p < 0.01$, $****p < 0.0001$.

ever, this did not reach statistical significance for any Treg subset (data not shown). Thus, freshly isolated CD226⁺TIGIT⁻ T cells exhibit comparable ex vivo suppression when freshly isolated, yet differ in FOXP3-TSDR demethylation and cytokine production.

Protocols to generate expanded human Tregs are susceptible to outgrowth of non-Tregs and the potential for lineage instability (15, 41–43). Therefore, we analyzed the purity and suppressive activity of Tregs post in vitro expansion based on CD226 and TIGIT expression (Fig. 5A). Although the TIGIT⁺ fractions constituted the majority of Tregs isolated from PBMCs, we observed these cells were highly refractory to expansion, limiting the overall Treg yield (Fig. 5A). This decrease in proliferative capacity of the sorted TIGIT⁺ Tregs supports the role of TIGIT as an intrinsic negative regulator (22), and also reflects an enrichment of Ag-experienced (CD45RO⁺) cells with limited expansion capacity (32). In contrast, the TIGIT⁻ Treg fraction expanded robustly from a naive state.

To further assess the purity and functional capacity of these subsets, we analyzed FOXP3 and Helios after expansion (Fig. 5B, 5C). The highest purity of postexpansion Tregs originated from cells lacking CD226 expression at the time of the initial sort (i.e., before in vitro expansion). The highest percentage of FOXP3⁺Helios⁺ cells was observed in the CD226⁻TIGIT⁺ population, followed by CD226⁻TIGIT⁻ and CD226⁺TIGIT⁺ cultures (90.73 ± 3.7, 83.69 ± 8.69, and 74.30 ± 10.13%, respectively). In contrast, the CD226⁺TIGIT⁻ population contained the least FOXP3⁺Helios⁺ cells post expansion (38.18 ±

11.70). Tconvs expanded with very little FOXP3 and Helios coexpression (Fig. 5B). In terms of surface CD226 and TIGIT expression, TIGIT was maintained or upregulated on TIGIT⁺ and TIGIT⁻CD226⁻ cells after expansion but remained low on TIGIT⁻CD226⁺ Treg and Tconv populations (Fig. 5D, 5E).

We previously demonstrated that expanded Tregs from T1D subjects were enriched in FOXP3⁺Helios⁻ cells with the capacity to produce IFN-γ (32). Accordingly, CD226⁺ Tregs have increased capacity to produce IFN-γ upon stimulation, whereas CD226⁻ Tregs were almost completely devoid of IFN-γ (Fig. 5F, 5G). CD226⁻ Tregs (TIGIT⁺ or TIGIT⁻) were both able to potently suppress autologous CD4 and CD8 T cell proliferation, with some diminution observed in the CD226⁺ expanded subset (Fig. 5H). The CD226⁻TIGIT⁻ and CD226⁻TIGIT⁺ subsets were almost completely demethylated at the TSDR (92.0 ± 3.13 and 94.5 ± 3.71%, respectively; Fig. 5I). The degree of demethylation at the TSDR correlated strongly with FOXP3 and Helios coexpression determined by FACS ($R^2 = 0.94$, $p < 0.0001$; Fig. 5I).

CD226⁺TIGIT⁻ T cells express an activated effector gene expression profile and produce IL-10 and effector cytokines

Gene expression profiles provide a powerful signature of the regulatory and effector mechanisms used by T cells (8). Given that most Treg therapies will require some form of expansion, we conducted a gene profile on in vitro–expanded Tconvs (CD4⁺ CD25⁻CD127⁺) or Tregs (CD4⁺CD25⁺CD127⁻/lo) that were further subdivided based on initial TIGIT and CD226 expression (Fig. 6A). From this analysis, we found 159 genes differentially expressed between the groups ($p < 0.05$). These data are summarized in the heat map and dendogram (Fig. 6A and Supplemental Table II). The normalized transcript counts were used to cluster the genes. About 18.6% of the variance observed was attributable to individual subject variance, whereas the remainder segregated based on the initial sorted populations. Tconvs showed a clear demarcation from Tregs, with the CD226⁺TIGIT⁻ population demonstrating an intermediate expression profile between Tregs and Tconvs (Fig. 6A, *green bars*). Interestingly, the CD226⁺TIGIT⁺ population has a Treg signature highly enriched in negative regulators and immunoregulatory pathways (Fig. 6B–E). Despite this regulatory signature, it did not completely correlate with their suppressive capacity after in vitro expansion (Fig. 5H). This may imply that CD226 negatively impacts suppression, or may reflect a preferential outgrowth of non-Tregs by day 14, as indicated by the TSDR results (Fig. 5I). PCA analysis of Treg subsets demonstrated the CD226⁺TIGIT⁻ population shared some common features with Tconvs (Fig. 6F). An extensive multiplex cytokine profile of freshly isolated Tregs further confirmed the capacity of CD226⁺TIGIT⁻ T cells to produce a broad array of cytokines (Fig. 6G, 6H).

Exclusion of CD226⁺ eliminates unstable Tregs after in vitro expansion

Improving Treg stability and limiting contamination non-tTregs may be critical for future Treg therapies (44). Prior efforts demonstrated that CD226 expression, irrespective of initial TIGIT expression, resulted in a sizable fraction of cells that were reduced in suppressive activity and methylated at the TSDR (Fig. 5). In addition, we noted that the TIGIT⁺ population was highly refractory to expansion. Thus, we hypothesized that eliminating CD226⁺ cells during the initial sort would increase purity without significantly constraining the final cell yield (Fig. 7A). We observed that total Tregs and CD226⁻ Tregs expanded with comparable kinetics (Fig. 7B). Importantly, the purity of the Treg
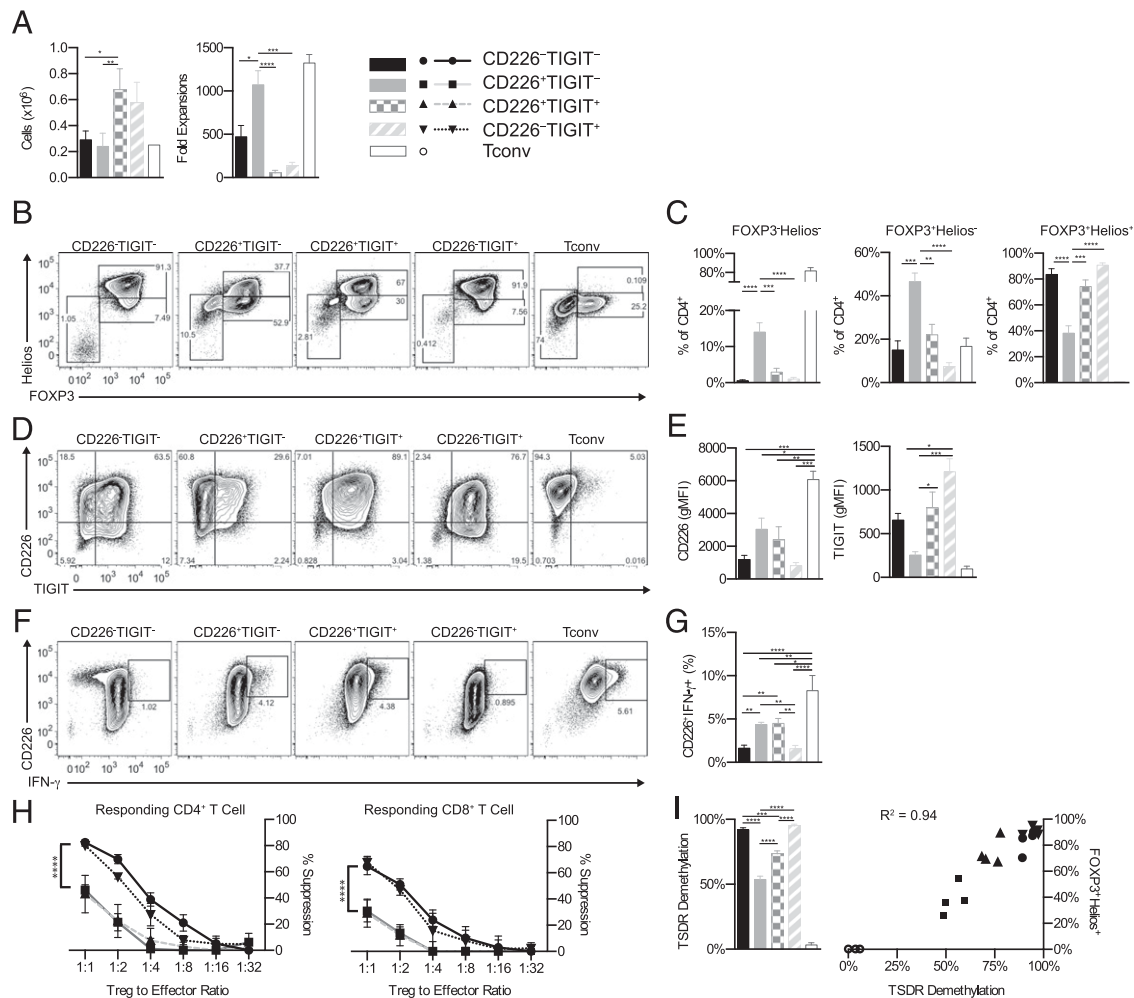
FIGURE 5. In vitro expansion of Tregs expressing TIGIT and/or CD226 yield subpopulations differing in proliferative ability, purity, and suppressive capacity. $CD4^+CD25^+CD127^{-/lo}$ Tregs were isolated from fresh peripheral blood and further divided to yield four distinct populations based on CD226 and TIGIT expression. (**A**) $TIGIT^+$ Tregs were refractory to expansion as the number of cells yielded on day 0 (*left graph*) was inversely related to fold expansion after 14 d of culture (*right graph*). After expansion, cells were reactivated with PMA/ionomycin for 4 h and assessed for FOXP3 and Helios (**B** and **C**), TIGIT and CD226 (**D** and **E**), and IFN-γ and CD226 (**F** and **G**). (**H**) The in vitro suppressive capacity of expanded Tregs was assessed. Percent suppression was calculated by division index of the $CD4^+$ or $CD8^+$ gated responder T cells in coculture relative to responders alone. (**I**) Graphs indicate the percent of cells demethylated at the FOXP3-TSDR (*left graph*), and the correlation between FOXP3-TSDR analysis and FOXP3 and Helios expression as analyzed by FACS after 14-d cultures (*right graph*; $R^2 = 0.94$, $p < 0.0001$). Data are represented as $\pm$SEM ($n = 4$). *$p < 0.05$, **$p < 0.01$, ***$p < 0.001$, ****$p < 0.0001$.

subsets ($FOXP3^+Helios^+$) was consistently higher in the $CD226^-$ Treg subset compared with the $CD226^+$ Treg fraction (89.33 ± 3.45 versus 57.2 ± 5.96, respectively; Fig. 7C, 7D). As noted previously, we again observed that CD226 expression correlated with IFN-γ (Fig. 7E, 7F). This observation was inversely related to TIGIT expression after culture (Fig. 7G, 7H). In terms of suppressive capacity, $CD226^-$ Tregs were consistently more able to suppress $CD4^+$ and $CD8^+$ responder T cells than their $CD226^+$ Treg counterparts (Fig. 7I). Indeed, an increased ratio of TIGIT/CD226 expression on the tTreg population after an in vitro suppression assay was associated with increased suppressive activity and TSDR demethylation (Fig. 7I–K). Taken together, these results suggest that elimination of cells expressing CD226 provides an effective means to further enrich a stable population of human Tregs.

Discussion

Prior efforts to define the transcriptional profile of human Tregs have relied primarily upon the use of surrogate surface markers for isolation. This methodology is subject to alterations in surface marker expression after Ag exposure and cellular activation (particularly for CD45RA, CD25, and CD127). In our study, we conducted a direct transcriptional profile of Tregs by FACS sorting cells based on the transcription factors FOXP3 and Helios. This analysis identified TIGIT, an important negative regulator, as highly expressed on tTregs relative to Tconvs or $FOXP3^+Helios^-$ T cells.

To further investigate this axis, we characterized TIGIT expression on Tregs in the context of the competing costimulatory molecule CD226. This analysis identified four distinct subpopulations of cells based on their surface expression of these receptors. Our results demonstrated CD226 expression marks both T_{CM} and T_{EM} and Treg subsets capable of producing IFN-γ and IL-10 for Tregs. Interestingly, TIGIT expression was stable or upregulated on Tregs after in vitro expansion. An incipient concept in Treg biology relates to the ability of Tregs to co-opt the transcription programs of the Th cells they are posed with suppressing (e.g., $Tbet^+$ Tregs suppress Th1 immunity [45], Th2-Tregs suppress humoral responses [46], and so on). It is intriguing to think this may also be the case for Ag-experienced Tregs
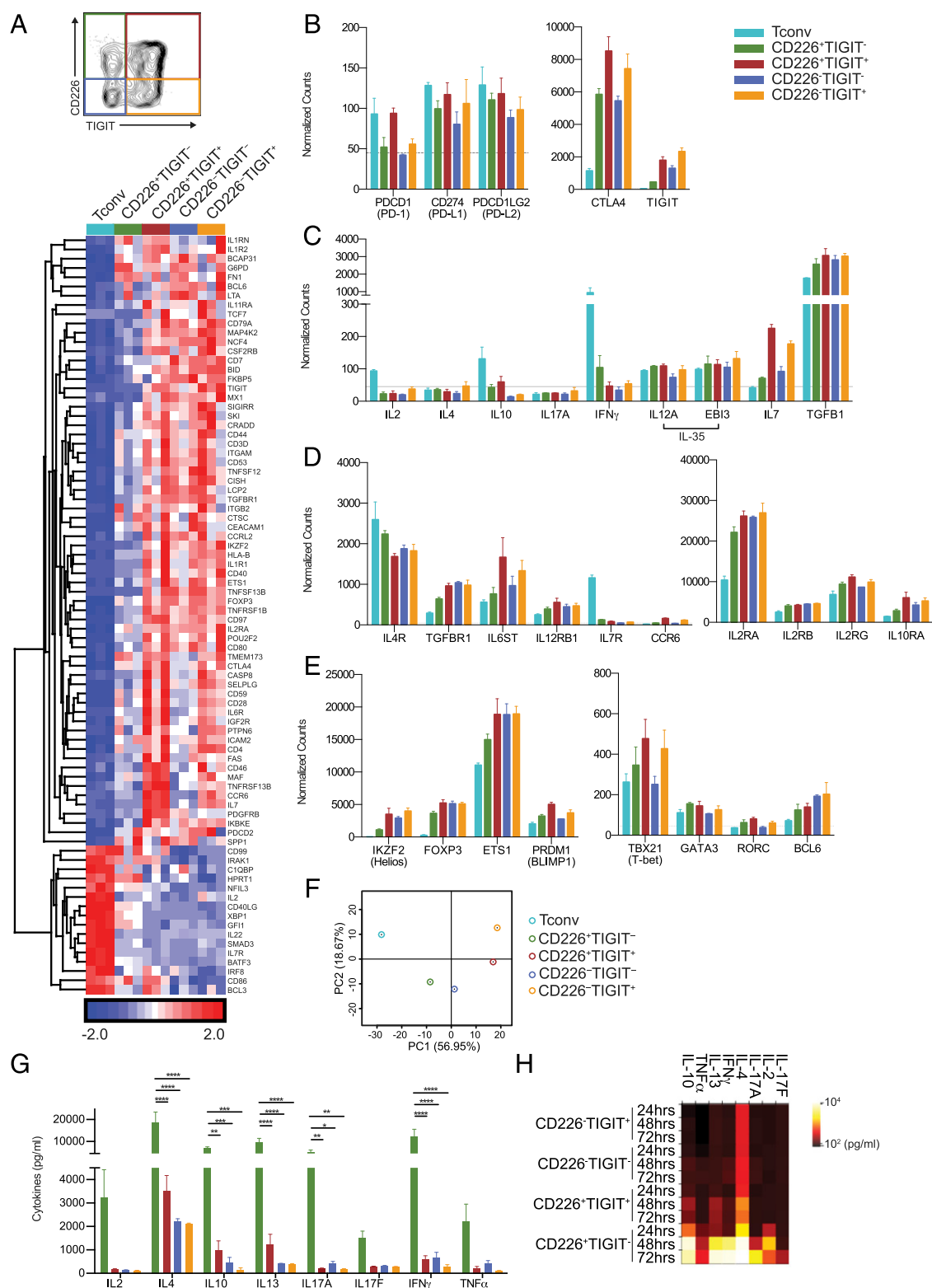
FIGURE 6. CD226^{+}TIGIT^{−} Tregs display an intermediate effector gene expression profile and produce cytokines. mRNA was isolated from 14-d in vitro–expanded Treg subsets and Tconvs and analyzed for gene expression on the Human Immunology GX Panel on the NanoString platform. (**A**) Treg and Tconv profiles shown by hierarchical clustering based on the Euclidian distance was used to create a heat map and dendrogram of the genes in Partek Genomic Suite. Select genes of interest are shown and grouped based on (**B**) coinhibitory receptors, (**C**) cytokines, (**D**) cytokine receptors or subunits, and (**E**) lineage-associated transcription factors. Normalized gene counts are represented as ±SEM with gray horizontal lines indicating the background expression threshold (*n* = 3). (**F**) The similarity of each Treg subset to Tconvs was shown by PCA analysis. (**G** and **H**) Fresh Treg subsets sorted according to CD226 and TIGIT expression were activated by CD3/28 dynabeads for 24, 48, and 72 h. Cytokine production was tested by multiplex assay and shown by bar graph and heat map. Data are represented as ±SEM (*n* = 4). *$p < 0.05$, **$p < 0.01$, ***$p < 0.001$, ****$p < 0.0001$.
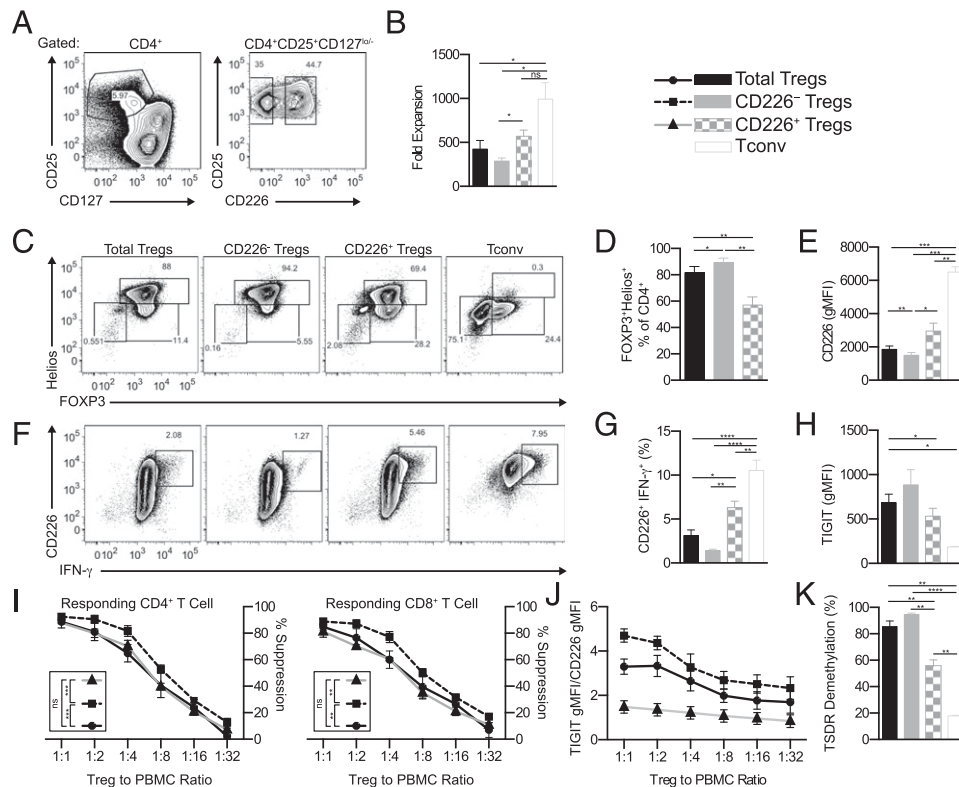
FIGURE 7. Exclusion of CD226$^+$ Tregs reduces IFN-γ production and augments the in vitro suppressive capacity of Tregs. (**A**) Total CD4$^+$CD25$^+$ CD127$^{lo/-}$ Tregs or CD4$^+$CD127$^-$ Tconvs were FACS sorted and Tregs were further subdivided into CD226$^+$ and CD226$^-$ subsets (*right plot*). (**B**) Cells were expanded for 14 d, rested to 21 d, and then reactivated with PMA/ionomycin for 4 h. Treg purity was assessed by FACS for (**C** and **D**) FOXP3 and Helios, (**E**) CD226 expression by gMFI, (**F** and **G**) IFN-γ and CD226 expression, and (**H**) TIGIT expression by gMFI. (**I**) CD226$^+$ and CD226$^-$ Treg subsets were assessed for their ability to suppress autologous CD4$^+$ or CD8$^+$ responder T cells from PBMCs. (**J**) The ratio of TIGIT and CD226 expression, as assessed by gMFI on gated Treg populations following the suppression assay (day 4). (**K**) Graph indicates the percent of cells demethylated at the FOXP3-TSDR. Data are represented as $\pm$SEM ($n = 4$). *$p < 0.05$, **$p < 0.01$, ***$p < 0.001$, ****$p < 0.0001$.

that are CD226$^+$TIGIT$^+$. In support of this, we noted lineage-associated chemokine receptor expression on both CD226- and TIGIT-expressing Tregs.

TIGIT$^+$CD226$^-$ Tregs expressed high levels of FOXP3 and Helios, and were demethylated at the TSDR. Moreover, data from in vitro suppression assays indicated TIGIT expression on Tregs was associated with robust suppressive activity. We would speculate the relative ratio of these receptors might provide an informative biomarker. These findings are particularly timely given the genetic associations of *CD226* in autoimmune diseases (11, 12, 18) and multiple reports of Treg functional defects and effector cytokine production by Tregs (e.g., IFN-γ and IL-17). Interestingly, analysis of IL-10–producing T regulatory type 1 cells also reported high CD226 expression, in addition to CD49b and LAG3 (47).

Our findings for TIGIT$^+$ Tregs draw some distinctions from those recently reported by Joller et al. (31), who suggested TIGIT$^+$ Tregs share features with T cells of a proinflammatory lineage. Our results indicate this phenotype may be more representative of cells coexpressing CD226 and TIGIT, as few cytokines or effector genes were upregulated in TIGIT single-positive populations. In fact, IL-10 expression and the IL-10–associated transactivator PRDM1 (48) were only discernible in the CD226$^+$TIGIT$^+$ Treg population. Moreover, the shift toward an effector-like lineage was most prominent in the CD226$^+$TIGIT$^-$ population.

Immunotherapeutics targeting coinhibitory molecules such as CTLA-4 and PD-1 have garnered increasing interest following notable clinical successes (49). Our findings raise important implications for future therapies that may seek to target the

CD226/TIGIT axis. Our studies support prior reports that CD226 is associated with proinflammatory Tconvs (21, 50). In addition, our data clearly demonstrate CD226 is also expressed at low to intermediate levels on naive T cells and may play a key role in IL-10–producing Tregs. Moreover, CD226 is upregulated on the majority of tTregs after activation. Thus, therapies seeking to block CD226 to attenuate Tconv activity must be carefully dosed to target CD226^{hi}-expressing Tconvs, whereas preserving naive T cells and IL-10–producing T regulatory type 1. Our results also suggest the CD226/TIGIT axis may be susceptible to control by innate inflammatory cytokines, as we demonstrated for IL-12. These findings suggest that one potential benefit of anti–IL-12 Ab therapy may be the preservation of TIGIT expression on tTregs. Finally, our study has implications for Treg adoptive cell therapies that are currently progressing in clinical trials for a number of autoimmune conditions (44). Overall, our studies continue to support the notion that CD4$^+$CD25$^+$CD127$^{-/lo}$ Tregs maintain a high degree of purity after expansion over a period of 14 d. Extending these findings, we demonstrated that the selection of the TIGIT$^+$ Treg population resulted in a highly enriched population, but this came at the cost of initial Treg recovery and resulted in a highly refractory population limiting the overall yield. However, our data also suggest that the isolation of CD226$^-$ Tregs, irrespective of initial TIGIT expression, results in a highly pure and potent population of TIGIT$^+$ Tregs for use in cell therapies. In summary, these data provide a biological context in which the autoimmune candidate gene *CD226* may modulate T cell biology. Moreover, these studies provide markers to identify highly suppressive Tregs for use in cell therapies.

Acknowledgments

Disclosures

Y.Z. D.v.S., Y.L., and M.W. are employees of Pfizer. The other authors have no financial conflicts of interest.

References

1. Bach, J. F. 2003. Autoimmune diseases as the loss of active "self-control". *Ann. N. Y. Acad. Sci.* 998: 161–177.
2. Asano, M., M. Toda, N. Sakaguchi, and S. Sakaguchi. 1996. Autoimmune disease as a consequence of developmental abnormality of a T cell subpopulation. *J. Exp. Med.* 184: 387–396.
3. Bennett, C. L., J. Christie, F. Ramsdell, M. E. Brunkow, P. J. Ferguson, L. Whitesell, T. E. Kelly, F. T. Saulsbury, P. F. Chance, and H. D. Ochs. 2001. The immune dysregulation, polyendocrinopathy, enteropathy, X-linked syndrome (IPEX) is caused by mutations of FOXP3. *Nat. Genet.* 27: 20–21.
4. Brusko, T. M., A. L. Putnam, and J. A. Bluestone. 2008. Human regulatory T cells: role in autoimmune disease and therapeutic opportunities. *Immunol. Rev.* 223: 371–390.
5. Fife, B. T., and J. A. Bluestone. 2008. Control of peripheral T-cell tolerance and autoimmunity via the CTLA-4 and PD-1 pathways. *Immunol. Rev.* 224: 166–182.
6. O'Shea, J. J., and W. E. Paul. 2010. Mechanisms underlying lineage commitment and plasticity of helper CD4+ T cells. *Science* 327: 1098–1102.
7. Yang, X. P., K. Ghoreschi, S. M. Steward-Tharp, J. Rodriguez-Canales, J. Zhu, J. R. Grainger, K. Hirahara, H. W. Sun, L. Wei, G. Vahedi, et al. 2011. Opposing regulation of the locus encoding IL-17 through direct, reciprocal actions of STAT3 and STAT5. *Nat. Immunol.* 12: 247–254.
8. Ferraro, A., A. M. D'Alise, T. Raj, N. Asinovski, R. Phillips, A. Ergun, J. M. Replogle, A. Bernier, L. Laffel, B. E. Stranger, et al. 2014. Interindividual variation in human T regulatory cells. *Proc. Natl. Acad. Sci. USA* 111: E1111–E1120.
9. Bailey-Bucktrout, S. L., and J. A. Bluestone. 2011. Regulatory T cells: stability revisited. *Trends Immunol.* 32: 301–306.
10. Buckner, J. H. 2010. Mechanisms of impaired regulation by CD4(+)CD25(+) FOXP3(+) regulatory T cells in human autoimmune diseases. *Nat. Rev. Immunol.* 10: 849–859.
11. McClymont, S. A., A. L. Putnam, M. R. Lee, J. H. Esensten, W. Liu, M. A. Hulme, U. Hoffmüller, U. Baron, S. Olek, J. A. Bluestone, and T. M. Brusko. 2011. Plasticity of human regulatory T cells in healthy subjects and patients with type 1 diabetes. *J. Immunol.* 186: 3918–3926.
12. Dominguez-Villar, M., C. M. Baecher-Allan, and D. A. Hafler. 2011. Identification of T helper type 1-like, Foxp3+ regulatory T cells in human autoimmune disease. *Nat. Med.* 17: 673–675.
13. Beriou, G., C. M. Costantino, C. W. Ashley, L. Yang, V. K. Kuchroo, C. Baecher-Allan, and D. A. Hafler. 2009. IL-17-producing human peripheral regulatory T cells retain suppressive function. *Blood* 113: 4240–4249.
14. Smilek, D. E., M. R. Ehlers, and G. T. Nepom. 2014. Restoring the balance: immunotherapeutic combinations for autoimmune disease. *Dis. Model. Mech.* 7: 503–513.
15. Sakaguchi, S., M. Miyara, C. M. Costantino, and D. A. Hafler. 2010. FOXP3+ regulatory T cells in the human immune system. *Nat. Rev. Immunol.* 10: 490–500.
16. Thornton, A. M., P. E. Korty, D. Q. Tran, E. A. Wohlfert, P. E. Murray, Y. Belkaid, and E. M. Shevach. 2010. Expression of Helios, an Ikaros transcription factor family member, differentiates thymic-derived from peripherally induced Foxp3+ T regulatory cells. *J. Immunol.* 184: 3433–3441.
17. Bottino, C., R. Castriconi, D. Pende, P. Rivera, M. Nanni, B. Carnemolla, C. Cantoni, J. Grassi, S. Marcenaro, N. Reymond, et al. 2003. Identification of PVR (CD155) and Nectin-2 (CD112) as cell surface ligands for the human DNAM-1 (CD226) activating molecule. *J. Exp. Med.* 198: 557–567.
18. Qiu, Z. X., K. Zhang, X. S. Qiu, M. Zhou, and W. M. Li. 2013. CD226 Gly307Ser association with multiple autoimmune diseases: a meta-analysis. *Hum. Immunol.* 74: 249–255.
19. Reinards, T. H., H. M. Albers, D. M. Brinkman, S. S. Kamphuis, M. A. van Rossum, H. J. Girschick, C. Wouters, E. P. Hoppenreijs, R. K. Saurenmann, A. Hinks, et al. 2014. CD226 (DNAM-1) is associated with susceptibility to juvenile idiopathic arthritis. *Ann. Rheum. Dis*. doi: 10.1136/annrheumdis-2013-205138.
20. Joller, N., J. P. Hafler, B. Brynedal, N. Kassam, S. Spoerl, S. D. Levin, A. H. Sharpe, and V. K. Kuchroo. 2011. Cutting edge: TIGIT has T cell-intrinsic inhibitory functions. *J. Immunol.* 186: 1338–1342.
21. Levin, S. D., D. W. Taft, C. S. Brandt, C. Bucher, E. D. Howard, E. M. Chadwick, J. Johnston, A. Hammond, K. Bontadelli, D. Ardourel, et al. 2011. Vstm3 is a member of the CD28 family and an important modulator of T-cell function. *Eur. J. Immunol.* 41: 902–915.
22. Lozano, E., N. Joller, Y. Cao, V. K. Kuchroo, and D. A. Hafler. 2013. The CD226/CD155 interaction regulates the proinflammatory (Th1/Th17)/anti-inflammatory (Th2) balance in humans. *J. Immunol.* 191: 3673–3680.
23. de Andrade, L. F., M. J. Smyth, and L. Martinet. 2014. DNAM-1 control of natural killer cells functions through nectin and nectin-like proteins. *Immunol. Cell Biol.* 92: 237–244.
24. Shibuya, K., J. Shirakawa, T. Kameyama, S. Honda, S. Tahara-Hanaoka, A. Miyamoto, M. Onodera, T. Sumida, H. Nakauchi, H. Miyoshi, and A. Shibuya. 2003. CD226 (DNAM-1) is involved in lymphocyte function-associated antigen 1 costimulatory signal for naive T cell differentiation and proliferation. *J. Exp. Med.* 198: 1829–1839.
25. Liu, S., H. Zhang, M. Li, D. Hu, C. Li, B. Ge, B. Jin, and Z. Fan. 2013. Recruitment of Grb2 and SHIP1 by the ITT-like motif of TIGIT suppresses granule polarization and cytotoxicity of NK cells. *Cell Death Differ.* 20: 456–464.
26. Lozano, E., M. Dominguez-Villar, V. Kuchroo, and D. A. Hafler. 2012. The TIGIT/CD226 axis regulates human T cell function. *J. Immunol.* 188: 3869–3875.
27. Bin Dhuban, K., E. d'Hennezel, E. Nashi, A. Bar-Or, S. Rieder, E. M. Shevach, S. Nagata, and C. A. Piccirillo. 2015. Coexpression of TIGIT and FCRL3 identifies Helios+ human memory regulatory T cells. *J. Immunol.* 194: 3687–3696.
28. Zhang, Y., J. Maksimovic, G. Naselli, J. Qian, M. Chopin, M. E. Blewitt, A. Oshlack, and L. C. Harrison. 2013. Genome-wide DNA methylation analysis identifies hypomethylated genes regulated by FOXP3 in human regulatory T cells. *Blood* 122: 2823–2836.
29. Yu, X., K. Harden, L. C. Gonzalez, M. Francesco, E. Chiang, I. Tom, S. Ivelja, C. J. Refino, H. Clark, et al. 2009. The surface protein TIGIT suppresses T cell activation by promoting the generation of mature immunoregulatory dendritic cells. *Nat. Immunol.* 10: 48–57.
30. Johnston, R. J., L. Comps-Agrar, J. Hackney, X. Yu, M. Huseni, Y. Yang, S. Park, V. Javinal, H. Chiu, B. Irving, et al. 2014. The immunoreceptor TIGIT regulates antitumor and antiviral CD8(+) T cell effector function. *Cancer Cell* 26: 923–937.
31. Joller, N., E. Lozano, P. R. Burkett, B. Patel, S. Xiao, C. Zhu, J. Xia, T. G. Tan, E. Sefik, V. Yajnik, et al. 2014. Treg cells expressing the coinhibitory molecule TIGIT selectively inhibit proinflammatory Th1 and Th17 cell responses. *Immunity* 40: 569–581.
32. Putnam, A. L., T. M. Brusko, M. R. Lee, W. Liu, G. L. Szot, T. Ghosh, M. A. Atkinson, and J. A. Bluestone. 2009. Expansion of human regulatory T-cells from patients with type 1 diabetes. *Diabetes* 58: 652–662.
33. Brusko, T. M., M. A. Hulme, C. B. Myhr, M. J. Haller, and M. A. Atkinson. 2007. Assessing the in vitro suppressive capacity of regulatory T cells. *Immunol. Invest.* 36: 607–628.
34. Baron, U., S. Floess, G. Wieczorek, K. Baumann, A. Grützkau, J. Dong, A. Thiel, T. J. Boeld, P. Hoffmann, M. Edinger, et al. 2007. DNA demethylation in the human FOXP3 locus discriminates regulatory T cells from activated FOXP3(+) conventional T cells. *Eur. J. Immunol.* 37: 2378–2389.
35. Sivendran, S., R. Chang, L. Pham, R. G. Phelps, S. T. Harcharik, L. D. Hall, S. G. Bernardo, M. M. Moskalenko, M. Sivendran, Y. Fu, et al. 2014. Dissection of immune gene networks in primary melanoma tumors critical for antitumor surveillance of patients with stage II-III resectable disease. *J. Invest. Dermatol.* 134: 2202–2211.
36. Hill, J. A., M. Feuerer, K. Tash, S. Haxhinasto, J. Perez, R. Melamed, D. Mathis, and C. Benoist. 2007. Foxp3 transcription-factor-dependent and -independent regulation of the regulatory T cell transcriptional signature. *Immunity* 27: 786–800.
37. Lilleri, D., C. Fornara, M. G. Revello, and G. Gerna. 2008. Human cytomegalovirus-specific memory CD8+ and CD4+ T cell differentiation after primary infection. *J. Infect. Dis.* 198: 536–543.
38. Zhao, J., J. Zhao, and S. Perlman. 2012. Differential effects of IL-12 on Tregs and non-Treg T cells: roles of IFN-γ, IL-2 and IL-2R. *PLoS ONE* 7: e46241.
39. Liu, W., A. L. Putnam, Z. Xu-Yu, G. L. Szot, M. R. Lee, S. Zhu, P. A. Gottlieb, P. Kapranov, T. R. Gingeras, B. Fazekas de St Groth, et al. 2006. CD127 expression inversely correlates with FoxP3 and suppressive function of human CD4+ T reg cells. *J. Exp. Med.* 203: 1701–1711.
40. Zheng, Y., S. Josefowicz, A. Chaudhry, X. P. Peng, K. Forbush, and A. Y. Rudensky. 2010. Role of conserved non-coding DNA elements in the Foxp3 gene in regulatory T-cell fate. *Nature* 463: 808–812.
41. Hoffmann, P., T. J. Boeld, R. Eder, J. Huehn, S. Floess, G. Wieczorek, S. Olek, W. Dietmaier, R. Andreesen, and M. Edinger. 2009. Loss of FOXP3 expression in natural human CD4+CD25+ regulatory T cells upon repetitive in vitro stimulation. *Eur. J. Immunol.* 39: 1088–1097.
42. Hoffmann, P., R. Eder, T. J. Boeld, K. Doser, B. Piseshka, R. Andreesen, and M. Edinger. 2006. Only the CD45RA+ subpopulation of CD4+CD25high T cells gives rise to homogeneous regulatory T-cell lines upon in vitro expansion. *Blood* 108: 4260–4267.
43. Zhou, X., S. Bailey-Bucktrout, L. T. Jeker, and J. A. Bluestone. 2009. Plasticity of CD4(+) FoxP3(+) T cells. *Curr. Opin. Immunol.* 21: 281–285.
44. Riley, J. L., C. H. June, and B. R. Blazar. 2009. Human T regulatory cell therapy: take a billion or so and call me in the morning. *Immunity* 30: 656–665.
45. Koch, M. A., K. R. Thomas, N. R. Perdue, K. S. Smigiel, S. Srivastava, and D. J. Campbell. 2012. T-bet(+) Treg cells undergo abortive Th1 cell differentiation due to impaired expression of IL-12 receptor β2. *Immunity* 37: 501–510.
46. Zheng, Y., A. Chaudhry, A. Kas, P. deRoos, J. M. Kim, T. T. Chu, L. Corcoran, P. Treuting, U. Klein, and A. Y. Rudensky. 2009. Regulatory T-cell suppressor program co-opts transcription factor IRF4 to control T(H)2 responses. *Nature* 458: 351–356.
47. Gagliani, N., C. F. Magnani, S. Huber, M. E. Gianolini, M. Pala, P. Licona-Limon, B. Guo, D. R. Herbert, A. Bulfone, F. Trentini, et al. 2013. Coexpression

of CD49b and LAG-3 identifies human and mouse T regulatory type 1 cells. *Nat. Med.* 19: 739–746.

48. Cretney, E., A. Xin, W. Shi, M. Minnich, F. Masson, M. Miasari, G. T. Belz, G. K. Smyth, M. Busslinger, S. L. Nutt, and A. Kallies. 2011. The transcription factors Blimp-1 and IRF4 jointly control the differentiation and function of effector regulatory T cells. *Nat. Immunol.* 12: 304–311.

49. Callahan, M. K., and J. D. Wolchok. 2013. At the bedside: CTLA-4- and PD-1-blocking antibodies in cancer immunotherapy. *J. Leukoc. Biol.* 94: 41–53.

50. Ardolino, M., A. Zingoni, C. Cerboni, F. Cecere, A. Soriani, M. L. Iannitto, and A. Santoni. 2011. DNAM-1 ligand expression on Ag-stimulated T lymphocytes is mediated by ROS-dependent activation of DNA-damage response: relevance for NK-T cell interaction. *Blood* 117: 4778–4786.